Thermal boundary layer effects on the acoustical impedance of enclosures and consequences for acoustical sensing devices[a)]

Stephen C. Thompson[b)]
Applied Research Laboratory, The Pennsylvania State University, P.O. Box 30, State College, Pennsylvania 16804

Janice L. LoPresti
Knowles Electronics, LLC, 1151 Maplewood Drive, Itasca, Illinois 60143

(Received 13 August 2007; revised 9 December 2007; accepted 11 December 2007)

Expressions are derived for the acoustical impedance of a rectangular enclosure and of a finite annular cylindrical enclosure. The derivation is valid throughout the frequency range in which all dimensions of the enclosure are much less than the wavelength. The results are valid throughout the range from adiabatic to isothermal conditions in the enclosure. The effect is equivalent to placing an additional, frequency-dependent complex impedance in parallel with the adiabatic compliance. As the thermal boundary layer grows to fill the cavity, the reactive part of the impedance varies smoothly from the adiabatic value to the isothermal value. In some microphones, this change in cavity stiffness is sufficient to modify the sensitivity. The resistive part of the additional cavity impedance varies as the inverse square root of frequency at high frequencies where the boundary layer has not grown to fill the enclosure. The thermal modification gives rise to a thermal noise whose spectral density varies asymptotically as $1/f^{3/2}$ above the isothermal transition frequency.
 [DOI: 10.1121/1.2832314]

PACS number(s): 43.38.Ar, 43.38.Kb, 43.35.Ud [AJZ] Pages: 1364–1370

I. INTRODUCTION

The acoustical impedance of enclosed air volumes is important in determining the performance of many acoustic sensing devices. It is well understood, for example, that the stiffness of the air volume behind the diaphragm of a condenser microphone must be considered to understand its sensitivity and frequency response. In many cases, the adiabatic compliance of the enclosure is sufficient to describe the effect. In small enclosures and at low frequencies, the thermal boundary layer can become a significant fraction of the total volume of the enclosure, causing interesting modifications to the cavity impedance. This paper will discuss the calculation of the acoustical impedance of enclosures with special attention to the frequency dependence of the acoustic resistance. Expressions for the rectangular enclosure and the annular cylindrical enclosure are provided. These shapes find practical application as enclosures in acoustical sensing devices. An example is shown in which the use of these results provides an improved match to the measured sensitivity of a miniature microphone.

Daniels[1] has provided a solution for the impedance of a spherical enclosure, and a method for calculation of the impedance of enclosures of other geometries. This work will follow the methods of Daniels. We are concerned with a harmonic acoustic pressure excitation given by $pe^{j\omega t}$, superimposed on the static pressure p_0. The pressure gives rise to an oscillating temperature variation $Te^{j\omega t}$ in the volume of the enclosure superimposed on the ambient temperature T_0. Combining Daniels' Eqs. (4), (6), and (8), the impedance of the enclosure can be written as

$$Z = \frac{\gamma p_0}{j\omega V\left[\gamma - (\gamma - 1)\dfrac{\bar{T}}{T_a}\right]} = \frac{Z_a}{\left[\gamma - (\gamma - 1)\dfrac{\bar{T}}{T_a}\right]}, \tag{1}$$

where V is the volume of the enclosure; $\gamma = C_p/C_v$ is the ratio of specific heats for the gas in the enclosure; C_p is the specific heat at constant pressure; C_v is the specific heat at constant volume; $\bar{T}$ is the value of the oscillatory temperature amplitude in the enclosure averaged over the volume of the enclosure; $T_a = pT_0(\gamma - 1)/p_0\gamma$ is the oscillatory temperature variation assuming purely adiabatic compression; $C_0 = V/\gamma p_0$ is the adiabatic compliance of the enclosure (when $\bar{T} = T_a$); and $Z_a = 1/(j\omega C_0)$ is the adiabatic impedance of the enclosure.

In the limit of large enclosures where $\bar{T} = T_a$, Eq. (1) reduces to the adiabatic impedance. For smaller enclosures, thermal transfer at the walls causes a significant spatial variation in T in the enclosure that modifies the impedance according to Eq. (1). If we set

$$Y = 1 - \frac{\bar{T}}{T_a} \tag{2}$$

then

[a)]Portions of this work were presented in "Acoustic noise in microphones from the thermal boundary layer resistance in enclosures," J. Acoust. Soc. Am. **119**, 3377 (2006).

[b)]Electronic mail: steve.thompson@psu.edu

$$Z = \frac{1}{j\omega C_0 + j\omega C_0(\gamma - 1)Y} = \frac{1}{\frac{1}{Z_a} + \frac{1}{Z_t}}, \tag{3}$$

which shows that the impedance can be represented as the parallel combination of the adiabatic impedance Z_a, and a thermal correction impedance Z_t given by

$$Z_t = \frac{1}{j\omega C_0(\gamma - 1)Y}, \tag{4}$$

which is caused by thermal transfer to the walls.

This separation of the total impedance into the adiabatic impedance and the thermal correction impedance is only a mathematical convenience, and is not meant to imply that these two impedances can be associated with separate regions of the enclosure volume. Equation (3) is convenient because it allows the impedances to be discussed as if they were to actual impedances connected in parallel. In particular it means that, in a frequency region where Z_a and Z_t differ in magnitude by a large factor, the larger value has a negligible effect on the magnitude of the total impedance.

Equation (1) shows that the cavity impedance can be calculated from the distribution of the oscillatory temperature amplitude in the enclosure. Daniels[1] shows that this temperature distribution can be found as a solution of

$$\nabla^2 T = \beta^2 (T - T_a) \tag{5}$$

where $\beta^2 = j\omega\rho_0 C_p/\kappa$; ρ_0 is the static density; and κ is the thermal conductivity of the gas in the cavity.

The general character of solutions to Eq. (5) can be illustrated in the simplest case of a semi-infinite space with a single isothermal boundary wall in the $z=0$ plane. It is straightforward to show that the solution is

$$T = T_a(1 - e^{-\beta z}) = T_a(1 - e^{-(1+j)z/\delta_\kappa}), \tag{6}$$

where

$$\delta_\kappa = \sqrt{\frac{2\kappa}{\omega\rho_0 C_p}} \tag{7}$$

is the thickness of the thermal boundary layer. Far from the wall, where $z \gg \delta_k$, the temperature variation is in phase with the acoustic pressure, and has its adiabatic value. Within the boundary layer the temperature variation decreases to zero at the wall, and there is a phase difference between the temperature and the pressure which approaches 45° at the wall. Figure 1 shows the magnitude and phase of the oscillatory temperature variation near an infinite wall for a frequency of 1 Hz. At other frequencies, Eq. (7) states that the thickness of the boundary layer varies inversely as the square root of frequency. The top axis in Fig. 1 shows T as a function of z/δ_κ.

Daniels[1] offered solutions for the temperature distribution and the enclosure impedance for three enclosure geometries in which T can be expressed as a function of a single spatial variable. These cases are a sphere, an infinite cylinder, and infinite parallel plates. Of these, only the sphere is truly an enclosure. The two idealized infinite cases can be seen as limiting cases for a cylinder much longer than its diameter

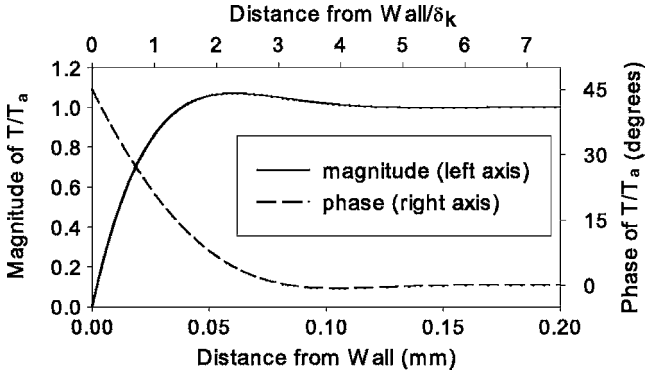

FIG. 1. Magnitude and phase of the oscillatory temperature variation near a wall. The frequency is 1 Hz.

and a thin flat enclosure whose cross-sectional dimensions are much larger than its thickness. A solution for the impedance of a finite cylinder was given by Biagi and Cook.[2] It can be shown that their expression for the impedance of a finite cylinder is limited properly to that for the infinite cylinder when the length is much greater than the radius, and to that for the infinite plates when the radius is much greater than the length. This paper gives solutions for the rectangular box and finite annular cylindrical enclosures.

II. THE SPHERICAL ENCLOSURE

To understand the nature of the enclosure impedance and its potential effect on sensor noise, one may use the example of the spherical enclosure. The temperature distribution in a spherical cavity is given by

$$\frac{T}{T_a} = 1 - \frac{\beta a}{\beta r}\frac{\sinh \beta r}{\sinh \beta a}, \tag{8}$$

where a is the radius of the sphere. Figure 2 shows the magnitude of the thermal distribution at several frequencies in a sphere with radius of 2 mm. Figure 3 shows the phase of this temperature distribution relative to the phase of the driving pressure. At higher frequencies where $\beta a \gg 1$, the boundary layer is confined to the region near the walls and the temperature approaches the adiabatic value through much of the volume. At low frequencies, however, the cavity becomes nearly isothermal at the wall temperature.

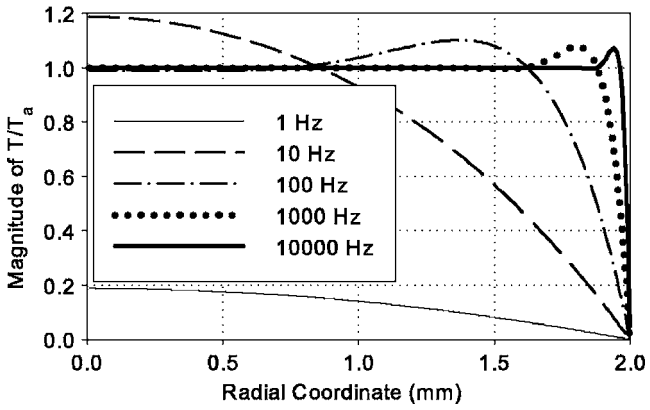

FIG. 2. Magnitude of the thermal distribution in a spherical cavity with radius 2 mm.

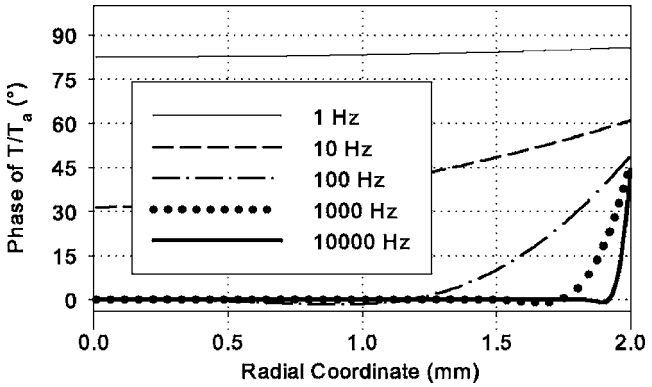

FIG. 3. Phase of the thermal distribution in a spherical cavity with radius 2 mm.

From Eqs. (2), (4), and (8), the thermal correction impedance is

$$Z_t = \frac{\beta^2 a^2}{3j\omega C_0(\gamma-1)(\beta a \coth \beta a - 1)}. \tag{9}$$

The real and imaginary parts of this expression are the resistance and reactance of the thermal correction impedance. The reactive impedance is shown in Fig. 4, and the resistance is shown in Fig. 5. The asymptotic behavior of the thermal correction impedance at low and high frequencies can be calculated from Eq. (9). At low frequencies,

$$Z_t \underset{\omega\to 0}{\to} \frac{1}{j\omega C_0(\gamma-1)} + \frac{a^2\rho_0 C_p}{15C_0(\gamma-1)\kappa}. \tag{10}$$

The resistive impedance is much smaller than the reactance, and can often be neglected. However, the resistance may be important in considering the noise generated by the enclosure impedance as will be discussed in Sec. V. The low frequency thermal reactance is a constant compliance in parallel with the adiabatic compliance according to Eq. (3). The two compliances in parallel create the isothermal compliance at low frequencies.

At high frequencies, Eq. (9) becomes

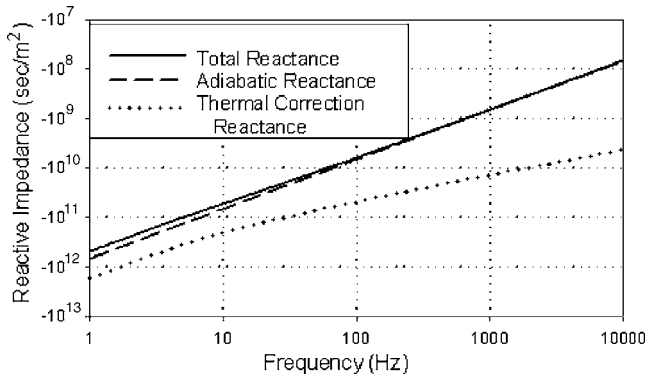

FIG. 4. The adiabatic impedance and the thermal correction impedance combine to yield the total impedance. Values are shown for a sphere of 2 mm radius.

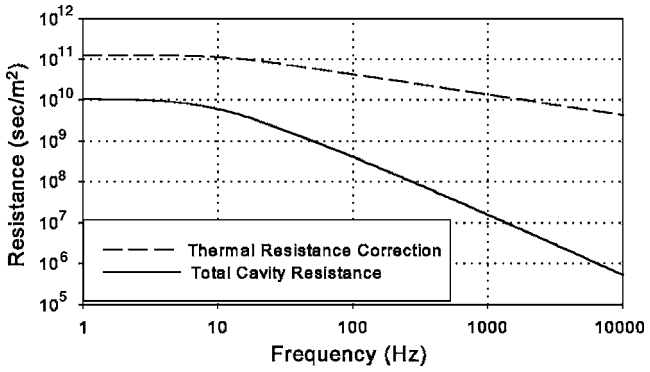

FIG. 5. The thermal correction resistance is constant at low frequencies and falls as $f^{-1/2}$ at high frequencies. The total cavity resistance falls as $f^{-3/2}$ at high frequencies. Values are shown for a sphere of 2 mm radius.

$$Z_t \underset{\omega\to\infty}{\to} \frac{V}{j\omega C_0(\gamma-1)S\delta_\kappa} + \frac{\gamma p_0}{\omega(\gamma-1)S\delta_\kappa}, \tag{11}$$

where S is the surface area of the enclosure. In Eq. (11), the magnitudes of the real and imaginary parts are equal, although they are written differently to facilitate the following explanation. Note that the boundary layer thickness δ_κ varies inversely as the square root of frequency so that at high frequencies, $Z_t \gg Z_a$. From Eq. (3), the much larger value of Z_t has a negligible effect on the total impedance. The thermal resistance is inversely proportional to the surface area of the enclosure and decreases as the square root of frequency. It has little effect on the magnitude of the total impedance, but the resistive loss may be important in determining the Q of a cavity at resonance, or in calculating the thermal noise in the enclosure. The dependence of the thermal resistance on the surface area is reasonable, because significant energy loss occurs only within the boundary layer. At high frequencies the boundary layer is confined to the surface, and the volume of the boundary layer is simply the surface area times the boundary layer thickness.

Note that in Eq. (11), the only reference to the geometry is the total volume and the total surface area. The authors believe that the equation in this form holds for any enclosure shape. This has been proven analytically for a sphere, for an infinite cylinder, and for infinite parallel plates. The numerical calculations in Sec. III show it to be true for a rectangular box of any aspect ratio. Figure 5 shows the thermal correction impedance and the total impedance for a sphere with radius 2 mm. At high frequencies the thermal correction resistance in Eq. (11) varies as $f^{-1/2}$ because of the implicit frequency dependence of δ_κ. By combining Eqs. (11) and (3) it can be shown that the total resistance at high frequencies varies as $f^{-3/2}$.

III. THE RECTANGULAR ENCLOSURE

Stinson[3] has provided a solution for the propagation of waves in a tube of rectangular cross section, including the effects of thermal transfer at the walls. The present derivation has much in common with that work. To find the temperature distribution in a rectangular enclosure with sides having lengths a, b, and c, we seek a solution to Eq. (5) with the boundary conditions

$$T = 0 \text{ when} \begin{cases} x = 0, & x = a \\ y = 0, & y = b \\ z = 0, & z = c. \end{cases} \tag{12}$$

The solution has the form

$$T = \sum_{\ell,m,n=1}^{\infty} A_{\ell mn} \sin \alpha_\ell x \sin \alpha_m y \sin \alpha_n z \tag{13}$$

where the boundary conditions require that

$$\alpha_\ell = \begin{cases} \dfrac{\ell \pi}{2a} & \text{when } \ell \text{ is odd} \\ 0 & \text{otherwise} \end{cases} \tag{14}$$

with similar expressions for α_m and α_n. To solve for the $A_{\ell mn}$, one should substitute Eqs. (13) and (14) into Eq. (5), multiply by the solution eigenfunction, and integrate over the volume of the enclosure. The full solution for the temperature distribution in the enclosure is then

$$\frac{T}{T_a} = \frac{64\beta^2}{\pi^3} \sum_{\ell,m,n=1,3,\ldots}^{\infty} \frac{\sin \alpha_\ell x \sin \alpha_m y \sin \alpha_n z}{\ell m n [\beta^2 + (\alpha_\ell^2 + \alpha_m^2 + \alpha_n^2)]} \tag{15}$$

and the average value of the temperature in the enclosure is

$$\frac{\bar{T}}{T_a} = \frac{512\beta^2}{\pi^6} \sum_{\ell,m,n=1,3,\ldots}^{\infty} \frac{1}{\ell^2 m^2 n^2 [\beta^2 + (\alpha_\ell^2 + \alpha_m^2 + \alpha_n^2)]}. \tag{16}$$

The value of Y in Eq. (2) is

$$Y = 1 - \frac{\bar{T}}{T_a} = \frac{512}{\pi^6} \sum_{\ell,m,n=1,3,\ldots}^{\infty} \frac{(\alpha_\ell^2 + \alpha_m^2 + \alpha_n^2)}{\ell^2 m^2 n^2 [\beta^2 + (\alpha_\ell^2 + \alpha_m^2 + \alpha_n^2)]}. \tag{17}$$

The thermal impedance of the rectangular enclosure is calculated by substituting this expression into Eq. (4). The total impedance of the enclosure is than calculated from Eq. (3). These calculations have been done numerically for five rectangular enclosures that have the same surface area. The first is a 4 mm cube. The others have thicknesses of 2, 1, 0.5, and 0.25 mm. The areas of the two square surfaces of each enclosure are adjusted to provide the same surface area, 96 mm^2. Figure 6 shows the total reactive impedances of the enclosures with the largest volume (the cube) and the smallest volume. These graphs show the same general behavior as the sphere, approaching the adiabatic value at high frequencies and approaching the isothermal value for low frequencies. Figure 7 shows the total resistance and the thermal correction resistance for the five rectangular enclosures. The thermal correction resistances for all of these enclosures have the same high frequency limiting behavior. Not only do the impedances fall with frequency at the same rate, they also have the same impedance value. This supports the statement in Sec. II that Eq. (11) holds for enclosures of any shape.

As the frequency is decreased, the resistance increases until the boundary layer has grown to fill the enclosure. When the cavity has become approximately isothermal, the resistance is constant with further decrease in frequency. The high frequency asymptotic behavior of the rectangular enclosure has the same frequency dependence as the spherical enclosure; namely, that the thermal correction resistance varies as $f^{-1/2}$ and the total resistance varies as $f^{-3/2}$.

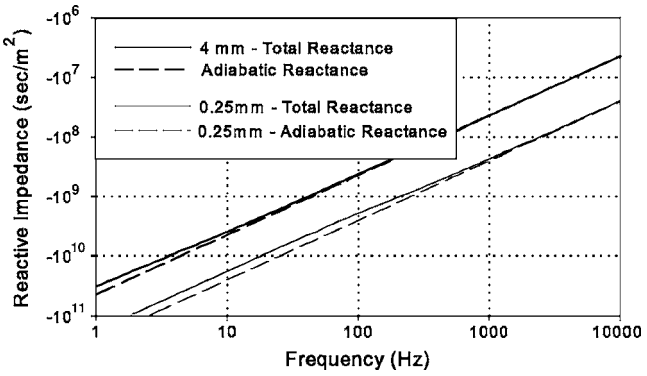

FIG. 6. The total reactive impedance of two different rectangular enclosures that have the same surface area.

IV. THE ANNULAR CYLINDRICAL ENCLOSURE

The right annular cylinder is a shape that is used as the internal volume of some commercial microphones. To calculate the acoustical impedance of this enclosure, we seek a solution to Eq. (5) in cylindrical coordinates with boundary conditions

$$T(r, \phi, z) = 0 \text{ when} \begin{cases} r = r_i, & r = r_o \\ z = 0, & r = 2b \end{cases}. \tag{18}$$

The complete formal method of solution can be found in standard mathematical references such as Hayek.[4] The solution has the form

$$T = \sum_{m,n=1}^{\infty} \left(A_{\text{mn}} J_0\left(\frac{\alpha_m r}{r_o}\right) + B_{mn} Y_0\left(\frac{\alpha_m r}{r_o}\right) \right) \times (\sin k_n z + D_n \cos k_n z). \tag{19}$$

The boundary conditions in z require that $D_n = 0$ and $k_n = n\pi z / 2b$. The radial boundary conditions require

$$A_{mn} J_0(\alpha_m) + B_{mn} Y_0(\alpha_m) = 0,$$

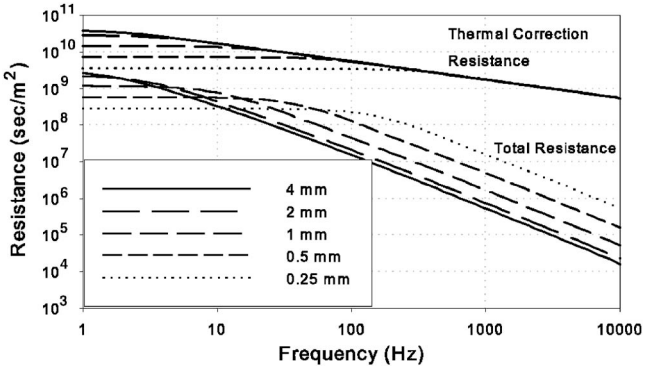

FIG. 7. The thermal resistance of a family of rectangular enclosures with 96 mm surface area. Two sides of the box are squares. The legend gives the thickness of the box.

$$A_{mn}J_0(\sigma\alpha_m) + B_{mn}Y_0(\sigma\alpha_m) = 0, \tag{20}$$

where

$$\sigma = \frac{r_i}{r_o}. \tag{21}$$

In order for Eq. (15) to have a nontrivial solution, it is necessary that

$$J_0(\alpha_m)Y_0(\sigma\alpha_m) - J_0(\sigma\alpha_m)Y_0(\alpha_m) = 0. \tag{22}$$

The radial eigenvalues α_m are the roots of this equation. These roots are tabulated for some values of σ, but must be calculated numerically in the general case. From Eq. (22) we may write

$$\frac{J_0(\alpha_m)}{Y_0(\alpha_m)} = \frac{J_0(\sigma\alpha_m)}{Y_0(\sigma\alpha_m)} = C_m. \tag{23}$$

The boundary conditions then allow the calculation of B_{mn} as

$$B_{mn} = -A_{mn}C_m \tag{24}$$

and T becomes

$$T = \sum_{m,n=1}^{\infty} A_{mn}\left[J_0\left(\frac{\alpha_m r}{r_o}\right) - C_m Y_0\left(\frac{\alpha_m r}{r_o}\right)\right]\sin\frac{n\pi z}{2b}. \tag{25}$$

The procedure to determine the A_{mn} is

(1) substitute this expression for T into Eq. (5);
(2) multiply both sides of the resulting equation by the eigenfunction with indices $k\ell$;
(3) integrate over the volume of the annular enclosure, and;
(4) use the orthogonality of the eigenfunctions to solve for A_{mn}.

This process is straightforward, if tedious, and results in

$$A_{mn} = \frac{8\beta^2 T_a}{n\pi\alpha_m}\frac{1}{\left[\beta^2 + \left(\frac{\alpha_m}{r_o}\right)^2 + \frac{n^2\pi^2}{4b^2}\right][G_m(\alpha_m) + \sigma G_m(\sigma\alpha_m)]}, \tag{26}$$

where

$$G_m(\alpha_m) = J_1(\alpha_m) - C_m Y_1(\alpha_m). \tag{27}$$

The average of the temperature over the volume of the annulus is

$$\bar{T} = \frac{1}{\pi(r_o^2 - r_i^2)2b}\int_0^{2b}\int_0^a 2\pi r T dr dz = \frac{32\beta^2 T_a}{\pi^2(1-\sigma^2)} \times \sum_{m,n=1}^{\infty}\frac{1}{n^2\alpha_m^2}\frac{[G_m(\alpha_m) - \sigma G_m(\sigma\alpha_m)]}{\left[\beta^2 + \frac{\alpha_m^2}{r_o^2} + \frac{n^2\pi^2}{4b^2}\right][G_m(\alpha_m) + \sigma G_m(\sigma\alpha_m)]} \tag{28}$$

from which the impedance of the enclosure can be calculated using Eq. (1).

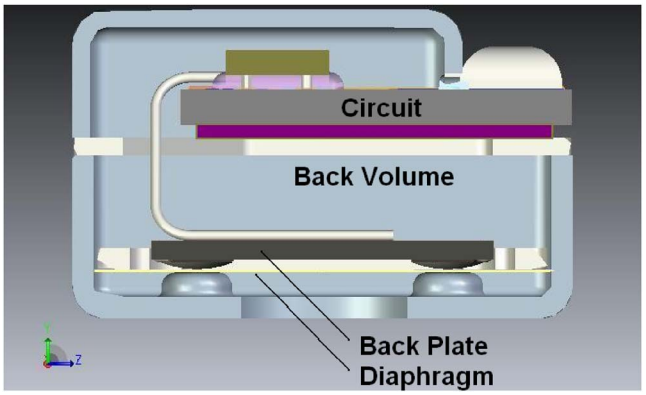

FIG. 8. (Color online) The microphone is a Knowles EM modified to have a single large hole in the case to admit sound to the diaphragm.

V. EFFECT ON SENSING DEVICES

The acoustical impedance of enclosed air volumes is important in determining the performance of many acoustic sensing devices. It is well understood, for example, that the stiffness of the air volume behind the diaphragm of a condenser microphone must be considered to understand its sensitivity and frequency response. Most often, however, the models used to calculate the performance of sensors use only the adiabatic compliance of the enclosure.[5–8] There are at least some cases in which the neglect of thermal effects leads to significant errors.

An example of this behavior is an experimental miniature microphone made by Knowles Electronics shown in Fig. 8. It is very similar to the "salt shaker" microphone previously described by Thompson *et al.*,[6] except that it has a single large hole in the case to admit sound pressure to the diaphragm. The internal construction of the microphone is that of the Knowles EM family. A cross section of this microphone is shown in Fig. 9. Sound enters the microphone through the large hole in the case at the bottom of Fig. 9. The diaphragm is suspended in front of an electret coated backplate, also sometime called the charge plate. The diaphragm is very thin and difficult to see in Fig. 8, but it is present at the position indicated. The thin air layer between the diaphragm and backplate is connected to the air in the backvolume by small channels that are not shown in Fig. 8. The

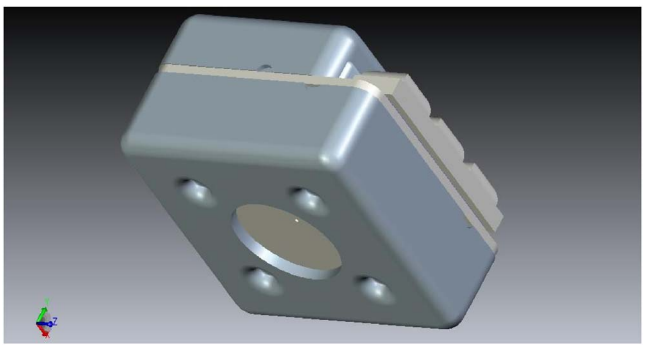

FIG. 9. (Color online) Cross section of the special microphone. The backvolume consists of two connected sections, one immediately above the backplate and the other near the top of the figure surrounding the amplifier circuit.

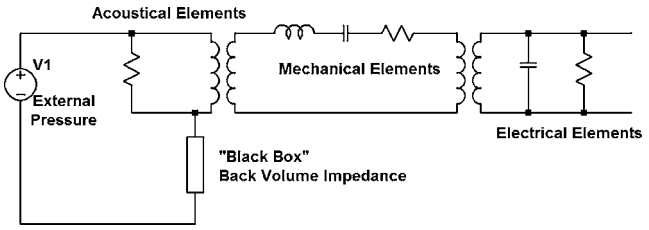

FIG. 10. The analog circuit model for the microphone has elements in the acoustical, mechanical, and electrical domains. The backvolume impedance, shown as a black box, is calculated by the methods of this paper.

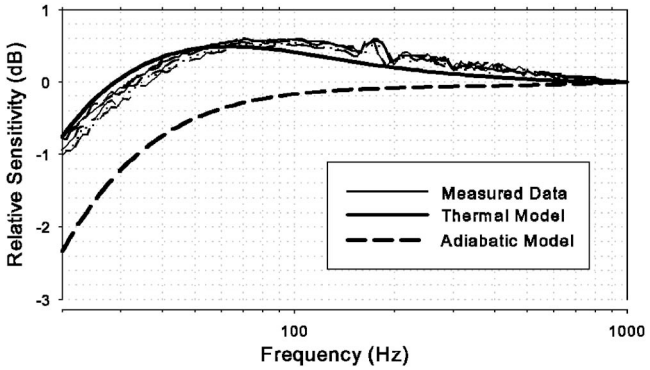

FIG. 11. Measured sensitivity data for five samples of the EM microphone compared with two theoretical calculations. The curve labeled "Adiabatic Model" uses only the adiabatic impedance for the backvolume. The curve labeled "Thermal Model" uses a numerical approximation to Eq. (17).

backvolume consists of two connected spaces above and below the circuit mounting plate. Each of these spaces is approximately rectangular. A wire connected to the backplate makes electrical connection to the amplifier chip mounted inside the backvolume. The diaphragm has a thin metallic coating to make it conductive, and this coating is electrically connected to ground potential. The diaphragm and backplate thus form the two plates of a capacitor whose output voltage drives the amplifier to produce the output signal.

The external acoustic pressure drives a small motion of the diaphragm. The diaphragm moves near the charged electret on the backplate and creates the signal voltage that is amplified to become the microphone output signal. The resistance of the air film between the diaphragm and backplate provides some damping to the motion of the diaphragm. The air film connects through holes at the edges and center of the diaphragm to the air contained in the microphone backvolume. There is also a small hole pierced in the diaphragm to equalize static pressure in the backvolume to the ambient air pressure.

The analog circuit that models the behavior of the microphone is shown in Fig. 10. The impedance analogy is used throughout the model. In the acoustical domain, the variables are acoustic pressure and volume velocity. As external pressure enters the microphone, a part of the volume flow goes through the diaphragm vent hole into the backvolume. The other part of the volume flow moves with the mechanical motion of the diaphragm. The acoustic flow through the vent and the diaphragm both enter the backvolume. The impedance of the backvolume is shown as a "black box" because, in general, it cannot be represented as a single simple component. Instead, the impedance of this backvolume enclosure should include the effects of thermal transfer as discussed in this paper. The acoustomechanical transformer in Fig. 10 performs the area transformation to the mechanical variables of force and velocity of the diaphragm. The mechanical elements represent the mass, compliance, and mechanical resistance of the diaphragm. The electromechanical transformer converts the diaphragm force and velocity into the electrical voltage and current that are the output of the microphone. The electrical terminals in Fig. 10 would normally be connected to an internal buffer amplifier which is not included here.

The thickness dimension of the open space in the backvolume is approximately 0.5 mm, although the actual thickness varies somewhat due to components on the circuit board and other assembly features of the microphone. Above approximately 300 Hz, the boundary layer thickness is a negligible fraction of the total enclosure thickness. Thus the adiabatic approximation should give an adequate model of the microphone behavior. Below 300 Hz, the effects of thermal transfer at the enclosure walls may become apparent. Figure 11 shows the low frequency sensitivity measured for the microphone compared with the model of Fig. 10. The midband sensitivity differences in the microphones have been removed in Fig. 11 by normalizing the responses to unity at 1 kHz. The model is calculated in two configurations. The first is using just the adiabatic compliance for the backvolume. The second uses a numerical approximation to the full expression of Eq. (17). Clearly the low frequency behavior is much better modeled when the thermal effects are included.

The change in microphone sensitivity from thermal effects is caused by the change in the compliance of the enclosure at low frequencies. The thermal resistance has little effect on the sensitivity. The thermal resistance could possibly affect the internal noise of the microphone if the noise from this resistance were comparable to or greater than the other thermal noise sources in the microphone. Figure 12 shows the frequency dependence of the total enclosure resistance for the microphone. The spectral density of the acoustic noise pressure from this resistance is[9]

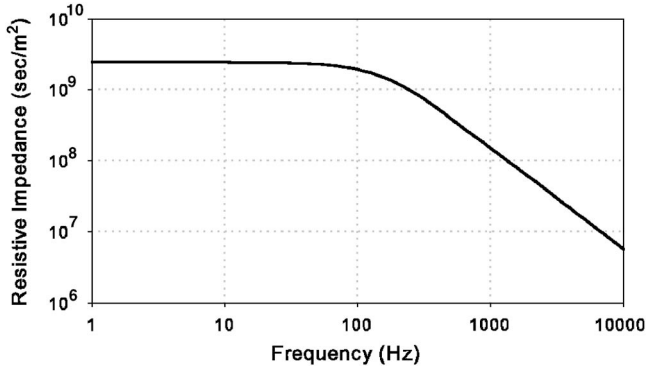

FIG. 12. The calculated enclosure resistance of the backvolume for the EM microphone.

$$N = \sqrt{4kT_0R}, \tag{29}$$

where k is Boltzmann's constant, T_0 is the ambient temperature, and R is the enclosure resistance. The noise voltage from this source is lower by more than an order of magnitude than that measured by Thompson *et al.* for essentially the same microphone. In this case, the thermal resistance of the enclosure has a negligible effect on the total internal noise of the microphone.

It is interesting to note, however, that the shape of the enclosure resistance curve of Fig. 12 is very similar to the shapes of the resistances of all of the other enclosure shapes calculated here. In particular, the low frequency asymptote is horizontal and the high frequency asymptote has the slope $f^{-3/2}$, and consequently the power spectral density of the noise it creates has the same asymptotic behavior. This noise is one of the sources present in any acoustic sensing device in which enclosed air volumes are present. In several studies, Zuckerwar and his colleagues have measured the acoustic noise present in a variety of acoustic sensors. In all cases, they have identified that the power spectral density of the acoustic noise at the low frequency limit of their measurement varies with frequency as f^{-1}. To date, no explanation has been offered for this spectral shape. The authors speculate that the thermal noise in the enclosed air spaces may be at least a part of the explanation for this spectral shape.

VI. CONCLUSIONS

This paper has reviewed the calculation of the acoustic impedance of enclosures and provided a new solution for the finite cylindrical annulus. The frequency-dependent change in acoustical compliance of the enclosure impedance can affect the sensitivity of some acoustic sensing devices for frequencies below that of the adiabatic to isothermal transition. The internal noise due to enclosure resistance is constant with frequency below the transition and falls as $f^{-3/2}$ above the transition.

ACKNOWLEDGMENTS

The authors would like to express deep gratitude to Sabih Hayek for discussions that were instrumental in the solution provided in Sec. IV. There have also been several helpful conversations with Daniel Warren, Steve Garrett, and Tom Gabrielson.

[1]F. B. Daniels, "Acoustical impedance of enclosures," J. Acoust. Soc. Am. **19**, 569–571 (1947).
[2]F. Biagi and R. K. Cook, "Acoustic impedance of a right circular cylindrical enclosure," J. Acoust. Soc. Am. **26**, 506–509 (1954).
[3]M. R. Stinson, "The propagation of plane sound waves in narrow and side circular tubes, and generalization to uniform tubes of arbitrary cross-sectional shape," J. Acoust. Soc. Am. **89**, 550–558 (1991).
[4]S. I. Hayek, *Advanced Mathematical Methods in Science and Engineering* (Dekker, New York, 2001), pp. 314, 336–342.
[5]A. J. Zuckerwar and K. C. Thi Ngo, "Measured $1/f$ noise in the membrane motion of condenser microphones," J. Acoust. Soc. Am. **95**, 1419–1425 (1994).
[6]S. C. Thompson, J. L. LoPresti, E. M. Ring, H. G. Nepomuceno, J. J. Beard, W. J. Ballad, and E. C. Carlson, "Noise in miniature microphones," J. Acoust. Soc. Am. **111**, 861–866 (2002).
[7]A. J. Zuckerwar, T. R. Kuhn, and R. M. Serbyn, "Background noise in piezoresistive, electret condenser, and ceramic microphones," J. Acoust. Soc. Am. **113**, 3179–3187 (2003).
[8]R. Dieme, Gijs Bosman, and Toshikazu Nishida, "Sources of excess noise in silicon piezoresistive microphones," J. Acoust. Soc. Am. **119**, 2710–2720 (2006).
[9]L. L. Beranek, *Acoustical Measurements* (Acoustical Society of America, Melville, 1993), p. 190.